EuroIntervention

Shear stress is associated with markers of plaque vulnerability and MMP-9 activity

R. Krams[1]*; C. Cheng[1]; F. Helderman[1]; S. Verheye[2]; L.C.A. van Damme[1]; B. Mousavi Gourabi[1]; D. Tempel[1]; D. Segers[1]; P. de Feyter[1]; G. Pasterkamp[3]; D. De Klein[3]; R. de Crom[4]; A.F.W. van der Steen[1]; P.W. Serruys[1]

1. Thorax center, Erasmus MC, Rotterdam, The Netherlands
2. Middelheim, Antwerp, Belgium
3. Department Experimental Cardiology Utrecht The Netherlands
4. Department of Vascular Surgery, Erasmus MC, Rotterdam, The Netherlands

All authors declare no conflict of interest.

KEYWORDS
Experimental atherosclerosis, vulnerable plaque, shear stress and CFD.

Abstract

Background: Vulnerable plaque has been associated with local macrophage accumulation and local high matrix metalloproteinase-2 (MMP-2) and MMP-9 activity. Since shear stress is a known local modulator of plaque location, we have determined whether local shear stress was associated with local plaque composition and with local MMP activity.

Methods and results: In 17 NZW rabbits plaque was generated by denudation of the infrarenal aorta over a region of 5 cm and feeding them a high cholesterol diet for 2 months. After 2 months, a motorised IVUS pullback of the infrarenal aorta was performed with a 40 MHz IVUS catheter (CVIS, Boston Scientific, USA). IVUS derived vessel wall-lumen contours were reconstructed in 3D with in-house developed software. These reconstructions served as an input for a computational fluid dynamics technique, from which the 3-D shear stress field was calculated. Plaque regions were divided in 5 regions (n=8) to identify the location of highest macrophage accumulation or selected on basis of shear stress to identify whether high shear stress selects macrophage accumulation (n=8). In a second series, shear stress values were used to select regions containing both latent and active MMP-2 and MMP-9. Segments were sectioned with a microtome and stained for smooth muscle cells (SMC), macrophages (MΦ) and collagen (COL). MΦ, displayed the highest density upstream of the plaque (6.9±2.4%, $p<0.05$), while SMC accumulated downstream (74.8±1.9%) of the plaque. High shear stress was associated with MΦ accumulation and MMP-9 activity ($p<0.05$).

Conclusion: Upstream location of macrophages in plaques is associated with high shear stress and MMP-9 accumulation. These findings are discussed in relation to rheological theories reported previously in atherosclerosis.

* Corresponding author: Experimental Echocardiography Laboratory, Thorax Center, Ee2369, Erasmus MC Rotterdam
Dr Molewaterplein 50, 3015 GE Rotterdam, The Netherlands
E-mail: r.krams@erasmusmc.nl

Introduction

Acute coronary syndromes have been associated most frequently with ruptured and superficially eroded plaques[1-3]. In search of the underlying mechanism, several groups have identified that ruptured plaques consist typically of a large lipid pool, covered with a thin fibrous cap and macrophages infiltrating the shoulder of these caps[2,4]. Recently, in addition to this cross-sectional characterisation of plaque composition, variation in the longitudinal composition of the human plaque has been reported[5-7]. The existence of both cross sectional and longitudinal heterogeneity is of importance, as local variation in plaque composition cannot be explained by systemic factors – such as existing risk factors for atherosclerosis – and thus local factors must be involved.

Variations in plaque location throughout the vascular system have been associated predominantly with local variation of shear stress[8-13]. We have developed and reported upon a technique to calculate local shear stress values with high resolution in human blood vessels[11-17]. For the present study we have modified this method, to evaluate the role of local shear stress (changes) on plaque heterogeneity in an experimental atherosclerotic rabbit model. With the combination of techniques we evaluate whether local shear stress plays a role in the local composition of plaques and thereby plaque rupture. As a special end-point, emphasis is placed upon markers of plaque vulnerability.

Recent studies proposed a relationship between inflammation and plaque vulnerability through the accumulation and activation of metalloproteinases[18,19]. MMPs in atherosclerotic plaques are synthesised by a variety of cells including endothelial cells, smooth muscle cells and (activated) macrophages[18,19]. Of the large family of MMPs, MMP-2 and MMP-9 have been associated with degradation of the basement membrane, cell migration and cell accumulation[19-21]. Furthermore, several studies showed that shear stress modulates the expression of MMP-2 and MMP-9 *in vitro* and *in vivo*[14,22,23]. Thus, to evaluate part of the underlying mechanism relating the accumulation of inflammatory cells to shear stress, we evaluated both latent and activated forms of MMP-2 and MMP-9 *in vivo*.

Methods

Instrumentation

All experiments have been performed in accordance with institutional regulations and the "Guiding principles for the care and use of animals" as approved by the Council of the American Physiological Society.

A couple of days before denudation, the rabbits started a high (2%) cholesterol diet, for a period of 2 months. On the day of experimentation, NZW rabbits (n=17; weight=3.1±0.2 kg) were premedicated with fentanyl (0.315 mg/ml) and fluanisone (10 mg/ml) (Hypnorm® 0.5 ml/kg i.m.) and anesthetised with propofol i.v. (10 mg/ml, infusion rate 10-15 ml/h, Abbott, Hoofddorp, The Netherlands), fentanyl i.a. (0.2 mg/kg/h, B.Braun, Melsungen, Germany) and a 2:1 mixture of N_2O:O_2 (vol/vol) after intubation (3.0 mm tube). The marginal ear artery was cannulated for arterial pressure measurement with a fluid-filled catheter (Amatek Inc., PA), and for arterial blood with drawal. The reduction in mean arterial blood pressure induced by the anaesthetics was compensated for by an infusion of adrenaline (1 mg/ml, infusion rate 2-12 ml/h, Centrafarm, Etten Leur, The Netherlands) titrated to achieve a mean arterial pressure of 70 mmHg. A 4 French guiding catheter was advanced from the arteriotomized femoral artery to the renal artery. After performing angiography, a 40 MHz IVUS catheter (CVIS, Boston Scientific, Maastricht, The Netherlands) was advanced through the guiding catheter and located just above the left renal artery. Next, a motorised pull back was performed at a speed of 0.5 mm/sec spanning an arterial segment of 7 cm, which included the denuded segment (see below). Subsequently, a Fogarty balloon (3F, Applied Medical, Laguna Hills, USA), attached to a manometer (2.2-2.5A) was located just below the renal artery and endothelial denudation was performed by pulling back and twisting the inflated Fogarty balloon three times over a length of 5 centimeter. After an 8-week follow up period, the right carotid artery was dissected for the introduction of a 5 French sheath. An angiographic overview image of the infra-renal aorta was carried out and markers were located to indicate the previously denuded region. A pull back was performed with the IVUS catheter as described above. Subsequently, the rabbit was euthanised (Euthasate®, 5 ml/kg) and perfusion fixation (formaldehyde 4%) was performed in the aorta under controlled arterial pressure of 70-80 mmHg for the duration of 20-30 minutes. Next, the infra-renal aorta was dissected and stored in 4% formaldehyde for further analysis.

3-D IVUS Reconstructions

3-D reconstruction of the infra-renal aorta before denudation and at follow up has been performed as follows. First, the IVUS images were digitised at intervals of 0.5 mm from the videotape with a resolution of 800×600 pixels and stored in a standard PC. Subsequently, the lumen and media were traced semi-automatically by a well-validated software package[17] and positioned perpendicular to the IVUS catheter axis at intervals of 0.5 mm. with in-house developed software (Matlab®, Mathworks Inc., Mass, USA). After resampling, a template deformable surface was fitted through the lumen and media contours such that a 3-D reconstruction of the lumen and wall of the iliac arteries was obtained. For comparison of the 3-D data set at baseline and at follow-up, the start (renal artery) and the end (5 cm) of the pull backs were aligned, and an interpolation algorithm was used to overlay both 3D reconstructions[11,12].

Computational fluid dynamics (CFD)

To obtain the 3-D shear stress distribution at follow up, the lumen of the reconstructed artery has been filled with 3-D finite elements with a method described previously[12]. The axial resolution of the mesh was 0.75±0.11 mm, while the cross-sectional resolution varied between 22 µm to 45 µm for the largest vessel diameter and between 9 to 19 µm for the smallest vessel diameter. The range of resolutions was a result of a purposely-induced increase in resolution towards the vessel wall. The boundary conditions for the CFD simulations consisted of a parabolic entrance velocity, no slip condition at the endothelium and zero stress at the outflow[12]. Blood was modelled as a non-Newtonian fluid[13]. Non-linear terms

of the Navier-Stokes relationships have been solved with a Newton-Raphson iteration scheme.

Tissue harvesting and histological analysis

All slices were stained with hematoxyline-eosine, and prepared for immunohistochemistry. Vessel morphology was obtained through the quantification of plaque area, medial area, and media bounded area from the hematoxyline-eosine stained slices with a software package (Clemex Technologies Inc., Quebec, Canada). In addition, monoclonal antibodies were applied to identify for macrophages (MΦ RAM-11, Dako Diagnostics BV, Glostrup, DK), and for smooth muscle cells (SMC: α-actin, Dako Diagnostics BV, Glostrup, DK). Collagen content was determined by picrosirius red (Sigma). Quantitative software has been developed applying the Clemex Vision software package. Areas of MΦ, SMC and COL were calculated and related to plaque area and reported as densities (%). On basis of these parameters an Vulnerability Index according to Saomi was calculated[25]. Four regions per cross section were studied and averaged to obtain a single number.

In the second series, zymography was performed as described previously[24]. Briefly, electrophoresis was performed applying 8% acrylamide gels containing 2mg/ml gelatin. Afterwards, the substrate gels were soaked twice with Triton X-100 solution for 30 minutes to remove SDS. The gels were then incubated in 50 mmol/L Tris-HCL, pH 7.4, 0.15 mol/L $CaCl_2$, 0.02%NaN_3, and 0.05% Brij 35 for 24 hours at 37 °C. The lyses of the substrates in the gels were visualized by staining with 2.5% Coomassie Brilliant Blue G-250 (Sigma Chemical Co.). Quantification was performed with a densitometric method.

Lipids

The plasma lipid profile (cholesterol, LDL-cholesterol, HDL-cholesterol and triglycerides) was measured according to well-established enzymatic-calorimetric methods (Roche Diagnostics, IN, USA) at 8 weeks follow up (n=9), and in a normocholesteremic control group (n=8).

Protocols

Two series of studies were performed. In the first series, the infra renal aorta was excised after perfusion-fixation and the plaque region divided into 5 equal regions (n=8) to identify the location of histological markers of plaque vulnerability. A second analysis on the first series was performed, by selection of the histological parameters on basis of high and low shear stress values (see below). This analysis aims at identifying the role of shear stress in plaque composition. In the second series, two 500 µm regions were selected in each plaque segment on basis of high, and low shear stress values, to study both latent and active MMP-2 and MMP-9 tissue content. This study was intended to study the relation between MMP activity and shear stress.

Analysis and statistics

The 3D shear stress tensor, obtained from the CFD simulations, was selected at the vessel wall and its magnitude was projected onto the vessel wall. Since no absolute entrance velocity was available in our experiments, the absolute shear stress values were divided by their vessel average and multiplied by 100% to obtain an Average Vessel Shear Stress (AVSS).

In order to spatially match the fixated arterial segment to the IVUS segment, we identified the start (renal artery) and the finish (5 cm) of the pull back in the arterial segment before sectioning. Then, the length of the vessel was measured directly after sectioning, and the ratio of both lengths was defined as a global shrinkage correction factor (GSCF). Next, the location of the arterial cross section was monitored and multiplied with the GSCF for correction of shrinkage in the histology. As we could not correct for rotational differences between both methods, all cross-sectional parameters were averaged per cross-section. From macrophage density (MΦ), smooth muscle cell density (SMC), and collagen distribution (COL), a VI-index[25], was calculated as MΦ/(SMC + COL). After that, the role of shear stress on plaque composition was evaluated by selection of all histology on basis of high (≥1.0*median), and low (<1.0*median) shear stress values in matched arterial segments.

In order to evaluate longitudinal cellular plaque heterogeneity, the value of each parameter (MΦ, SMC, COL, shear stress, plaque morphology, VI-index) was tested with ANOVA for repeated measures, taking location as the independent variable. To test the influence of shear stress, the two groups of MΦ, SMC, COL, shear stress, plaque morphology, VI-index and MMP-activity selected on basis of high and low shear stress were tested with a paired t-test. All values are reported as mean±SEM. A value of $P<0.05$ was considered significant.

Results

Animal characteristics

Arterial pressure was 85±5 mmHg and heart rate was 166±10 beats/min during denudation. A similar mean arterial pressure (84±3 mmHg) and heart rate (184±14) was measured at follow up. The plasma lipid profile changed significantly, as cholesterol increased to 33.9±12.4 mM (normal value: 1.4±0.2 mM; $p<0.05$); LDL-cholesterol to 28.7±9.2 (normal value: 0.2±0.1;$p<0.05$); HDL-cholesterol to 5.7±2.6 mM (normal value 0.7±0.1;$p<0.05$); and triglycerides to 32.2±21.5 mM (0.7±0.1;$P<0.05$). Normal values have been obtained from another group of rabbits (n=8).

Longitudinal heterogeneity of plaque composition

The longitudinal segments of the arteries that contained the atherosclerotic lesions were divided into 5 zones of equal length. Zone 1 and 2 represent the upstream shoulder region of the plaque, while zone 4 and 5 are the downstream shoulder region. Zone 3 is the pinnacle of the atherosclerotic lesion, containing the locations with the largest intimal areas of the various zones in all animals. Table 1 provides a detailed description of the vessel wall morphometry. Within the plaque region, the MΦ density (Figure 1) displayed its largest value upstream of the plaque (zone 2), while smooth muscle cells were located mainly downstream of the plaque (Figure 1). The entire group shows a similar result, as macrophage accumulation

Table 1. Histological derived vessel wall morphology and cellular distribution in 5 equidistant regions within the plaque of 8 rabbit aortas

	Zone 1	Zone 2	Zone 3	Zone 4	Zone 5
Vessel wall morphometry					
Plaque area (mm^2)	1.4±0.4	2.1±0.4	2.0±0.2	1.5±0.3	1.6±0.2
Media area (mm^2)	1.1±0.2	0.9±0.2	0.8±0.3	0.9±0.1	0.9±0.2
Lumen area (mm^2)	1.9±0.1	1.9±0.2	1.9±0.2	1.9±0.1	2.0±0.4
MBA (mm^2)	4.4±0.3	4.9±0.4	4.8±0.4	4.5±0.4	3.9.±0.4
Cellular and Shear Stress distribution in the plaque					
Macrophages (%)	2.5±1.4	6.9±2.4*	0.9±0.1	1.6±0.4	2.4±0.5
Smooth Muscle Cells (%)	64.4±2.2	62.9±3.4	70.7±4.4	74.8±1.9#	69.5±4.5
Collagen (%)	7.1±2.5	8.6±3.2	8.6±2.9	12.5±4.2	7.4±1.8
VI-index ($x10^{-2}$)	3.7±2.1	8.9±2.7*	1.1±0.2	1.8±0.5	3.2±0.8
Shear Stress (%)	109.5±9.9	106.2±6.3	103.1±7.4	95.6±8.1	85.7±6.8#

All values are mean ± standard error of the mean. * P<0.05, Zone is significantly different compared to any other location. # P<0.05, Zone is significantly different compared to Zone 1 and 2 (upstream).

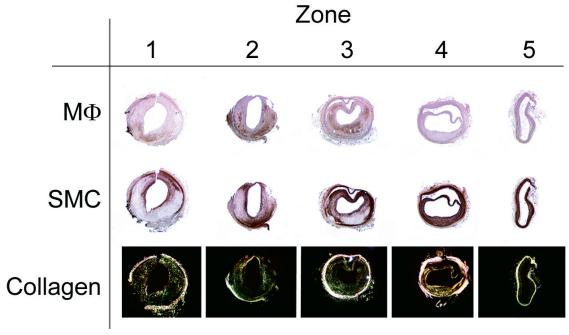

Figure 1. Example of Macrophage distribution (upper row), smooth muscle cell distribution (middle row) and collagen distribution versus location, where upstream is zone 1, and downstream is zone 5.

was increased up to 6.9±2.4% in zone 2 (Table 1). This was accompanied by a significant increase in SMC (74.8±1.9%) downstream of the plaque and an increased vulnerability index upstream of the plaque (8.9±2.7%; Table 1). Shift of MΦ vs. plaque area is apparent if both signals are scaled to 100% (Figure 2). A predominant downward shift is noted for collagen and the smooth muscle cells. These findings lead to a small upward shift of the vulnerability index (Figure 2).

Correlation of shear stress and plaque composition

After shear stress increased from 85.7% to 109.5% ($p<0.05$), macrophage density increased (to 344% of reference; $p<0.05$), smooth muscle cell density remained unchanged, collagen increased (to 154%) and the VI-index increased (from $2*10^{-2}$ to $4*10^{-2}$; $p=0.065$; Figure 3). Plaque area, media bounded area and medial area all remained unchanged after selection by shear stress (data not shown).

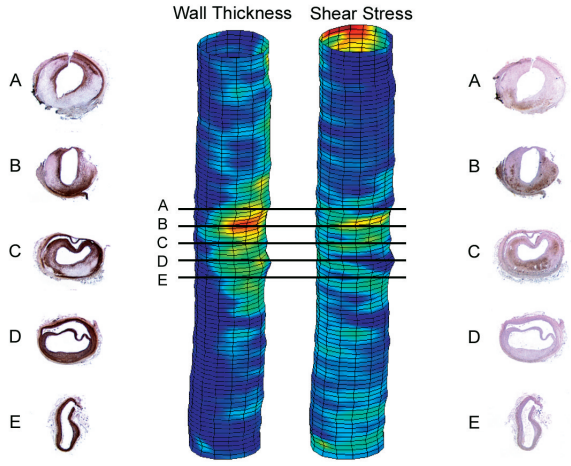

Figure 2. Typical wall thickness and shear stress distributions after 8 weeks of high cholesterol diet and endothelial denudation of the infrarenal aorta of a rabbit. Indicated are the smooth muscle cell distribution (left column) and macrophage distribution (right column). The black lines in the 3-D IVUS reconstruction indicate the location of these histological slides. Note that upstream macrophage predominantly accumulate while downstream the smooth muscle cells are predominant. The plaque in the cross-section shown at location D is dissected from the vessel wall as no lipids or MΦ can be indentified underneath the VSMC layer.

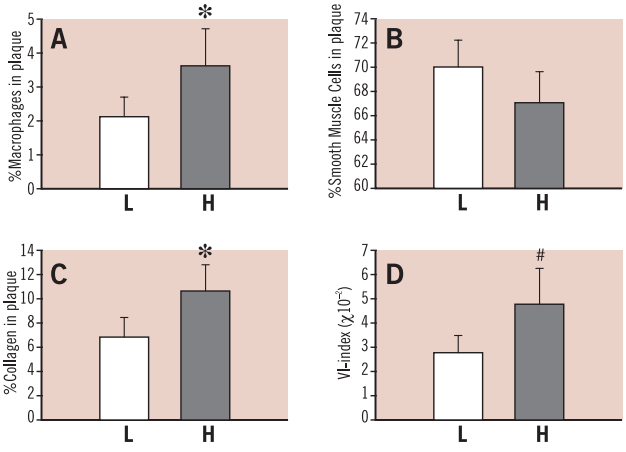

Figure 3. Accumulation of macrophages (Panel A), Smooth Muscle Cells (Panel B), Collagen (Panel C) and Vulnerability Index (Panel D) with respect to plaque location. L means Low shear stress, while H means high shear stress. Data were obtained by scaling each parameter from zero to 100 percent and to interpolate and smooth the individual measurement points by a linear interpolation scheme developed in Matlab.

Correlation of shear stress, MMP-2 and MMP-9 accumulation and activity

Latent MMP-2 (3.0±0.2 OD*mm^2 vs. 3.0±0.3 OD*mm^2), latent MMP-9 (0.6±0.01 OD*mm^2 vs. 0.7±0.02 OD*mm^2) and active MMP-2 (0.2±0.05 OD*mm^2 vs. 0.4±0.07 OD*mm^2) values were not different for low and high shear stress values respectively (Figure 4). In contrast active MMP-9 significantly increased from

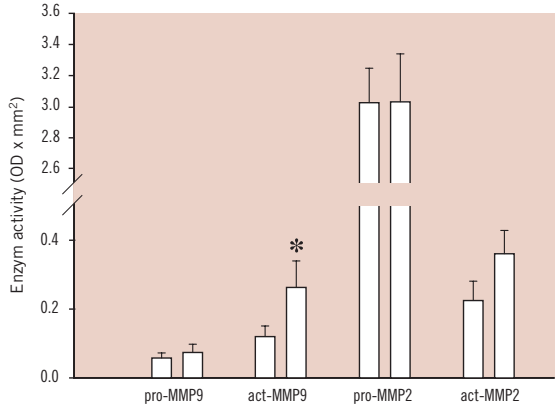

*Figure 4. Zymography-derived proMMP-2, active MMP-2, proMMP-9 and active MMP-9 selected on basis of low shear stress (black bars), and high shear stress (gray bars) values. * P<0.05 High shear versus low shear stress.*

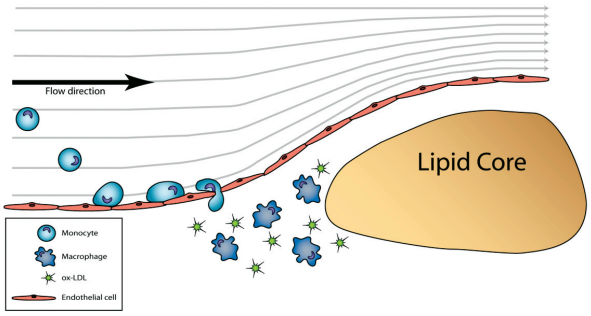

Figure 5. Postulated mechanism: Upstream of the plaque narrowing of the lumen induces curved flow lines, increments in velocity along the path (velocity gradients) and centrifugal derived velocity component directed towards the vessel wall. The combination of factors might enhance the interaction between particles and the vessel wall.

0.1±0.03 OD*mm^2 to 0.3±0.07 (OD*mm^2; p<0.05) units when these data were selected on basis of low and high shear stress values.

Discussion

Both plaque inflammation, plaque vulnerability and plaque rupture have been shown to be distributed heterogeneously in human plaques[5-7]. As classical risk factors are systemic of nature and cannot explain these local variations, we evaluated whether local shear stress might underlie these findings. The present study may be summarised as follows: i) plaques were generated in an animal model consisting of a predominantly upstream accumulation of macrophages, and a downstream accumulation of collagen and smooth muscle cells in the rabbit aorta. These findings are similar to those found in humans[5-7]; ii) local shear stress identified regions of high plaque vulnerability, and a high macrophage accumulation, suggesting a role of blood flow in plaque heterogeneity; and iii) high shear stress values were associated with high MMP-9 activity. Plaque vulnerability has been associated with a thin fibrous cap and with the existence of macrophages in the shoulder of the plaque[1,2,4]. Recently, in addition to this cross sectional heterogeneity of plaque composition, longitudinal heterogeneity of plaque composition was reported in human carotid arteries[5,7]. In those studies, comparable to the present study, SMC and collagen accumulation occurred predominantly downstream of the plaque, while macrophage accumulation occurred upstream of the plaque[5,7]. This finding is remarkable as, in general, high shear stress prevails upstream and low shear stress exists downstream of the plaque. Also in the present study high shear stress values occurred upstream, while low shear stress occurred downstream of the plaque. Low shear stress has been associated with VCAM-1 expression and macrophage adhesion[26,27] and cannot explain the present findings. However, in line with studies of Truskey et al[28] (Figure 5) we propose that the local rheological environment determines the interaction between macrophages and their adhesion factors and thereby the macrophage uptake. Factors that determine the local rheological environment are local velocity vectors directed towards the vessel wall ('secondary velocity patterns'[29]), long resident times, and gradients in shear stressor that increase local concentrations of macrophages[30]. All these factors determine the change of interaction between macrophages and the vessel wall. In addition, increased MMP-9 activity produced either by the endothelial layer or by previously accumulated macrophages may contribute to the subendothelial accumulation of monocytes in the plaque shoulder by locally increasing tissue permeability. However, the activation of chemokines, cytokines and other bio-active proteins that could prime the endothelium of the plaque for adhesion and transmigration of monocytes may have pivotal roles in this localised accumulation and should be further investigated in future studies.

Limitation of the method

Although the hypercholesteremic rabbit is a well-accepted model for the study of the vascular biology in atherosclerosis, it displays a relatively early form of atherosclerosis. As such extrapolations towards patients should be done with caution.

We did not measure, but calculated the shear stress distribution in the blood vessel. Although the method has been validated in several earlier studies by independent laboratories[11-15,17], it relies on a number of assumptions. We used parabolic inflow as entrance and constant, zero stress as outflow condition. We evaluated this effect in straight and curved tubes with Newtonian conditions[15]. It could be shown that 3-5 times the diameter (i.e. 10 mm) was necessary for compensating for these boundary effects. We evaluated, as described in the Methods section, only the plaque regions inside the denuded regions. We used a non-compliant wall for our calculations. In several studies it has been shown that a radial expansion of 2-7% which was measured in our experiments (data not shown) did not affect mean shear stress to a large extent.[31]

The current study is descriptive and limited to one time point at which the accumulation of different plaque components and lesion vulnerability is related to the actual shear stress conditions. It is impossible to analyse the same animal for shear stress conditions at several time points during development of the lesion using (immuno) histological parameters, because the animals need to be

sacrificed for analyses. Therefore, it is important to develop intravital imaging techniques to measure the various plaque components. For the matching of histological sections with our numerical package, we assume a homogeneous shrinkage of the blood vessel, despite a non-homogeneous distribution of plaque and lipids. Therefore, we introduced several markers upon the blood vessel at equidistant points in three aortas of atherosclerotic rabbits and measured their shrinkage before and after sectioning the 5 cm arterial segment. An overall shrinkage of 32% was accompanied by a variation of 1% (i.e. 0.3%) in individual sections (n=11), which is small compared to the overall effect.

We applied semi-quantitative techniques to obtain accumulation of cells into our plaque regions. To evaluate the reproducibility of this method, a random set of 10 slices was re-analysed by the same observer (to assess the inter-variability) and by a different observer blinded for the results of the first observer (to assess the intra-variability). The inter-variability for lumen, media and plaque areas was 0.09%, 0.11% and 1.93%, respectively, while for macrophage, smooth muscle and collagen accumulation it was 1.4%, 0.4% and 8.1%, respectively. The intra-variability for these lumen, media, plaque, macrophage, smooth muscle cell and collagen was 0.3%, 0.4%, 2%, 1%, 1% and 13%. Except for the collagen accumulation, the variability was small compared to the reported findings (see table 1). Denudation was a necessary step to create complex plaques in this animal model over such a short time period. To test for recurrence of the endothelial layer we performed a Von Willibrand staining for the 5 plaque regions obtained in series 1 (data not shown). For each segment Von Willibrand positive staining covered 63% of the circumference, independent of location within the plaque. Hence, re-endothelisation was uniform throughout the plaque and cannot explain the differences found in the plaque indicating that shear stress by itself might be an important factor.

Two series of studies were performed, as it was not possible in our hands to obtain histology and MMP activity in the same animal. This was due to the fact that zymography needed to be analysed in snap frozen tissue, excluding paraffin embedding, thereby reducing the morphological quality of the sections.

In conclusion, local increments in shear stress upstream of a plaque are associated with histological markers of plaque vulnerability and local MMP-9 activity. These findings suggest a relation between plaque vulnerability and local rheological conditions.

Acknowledgements

This study was supported by the Interuniversity Institute of Cardiology of the Netherlands (ICIN) (C. Cheng). Also R. Krams is a recipient of the established investigator grant of the Netherlands Heart Foundation.

References

1. Burke AP, Kolodgie FD, Farb A, Weber D, Virmani R. Morphological predictors of arterial remodeling in coronary atherosclerosis. *Circulation.* 2002;105:297-303.

2. Kolodgie FD, Burke AP, Farb A, Gold HK, Yuan J, Narula J, Finn AV, Virmani R. The thin-cap fibroatheroma: a type of vulnerable plaque: the major precursor lesion to acute coronary syndromes. *Curr Opin Cardiol.* 2001;16:285-292.

3. Libby P, Aikawa M. Stabilization of atherosclerotic plaques: new mechanisms and clinical targets. *Nat Med.* 2002;8:1257-1262.

4. Burke AP, Farb A, Malcom GT, Liang Y, Smialek JE, Virmani R. Plaque rupture and sudden death related to exertion in men with coronary artery disease. *Jama.* 1999;281:921-926.

5. Dirksen MT, van der Wal AC, van den Berg FM, van der Loos CM, Becker AE. Distribution of inflammatory cells in atherosclerotic plaques relates to the direction of flow. *Circulation.* 1998;98:2000-2003.

6. Tricot O, Mallat Z, Heymes C, Belmin J, Leseche G, Tedgui A. Relation between endothelial cell apoptosis and blood flow direction in human atherosclerotic plaques. *Circulation.* 2000;101:2450-2453.

7. Masawa N, Yoshida Y, Yamada T, Joshita T, Sato S, Mihara B. Three-dimensional analysis of human carotid atherosclerotic ulcer associated with recent thrombotic occlusion. *Pathol Int.* 1994;44:745-752.

8. Ku DN, Giddens DP, Zarins CK, Glagov S. Pulsatile flow and atherosclerosis in the human carotid bifurcation. Positive correlation between plaque location and low oscillating shear stress. *Arteriosclerosis.* 1985;5:293-302.

9. Traub O, Berk BC. Laminar shear stress: mechanisms by which endothelial cells transduce an atheroprotective force. *Arterioscler Thromb Vasc Biol.* 1998;18:677-685.

10. Zhao SZ, Ariff B, Long Q, Hughes AD, Thom SA, Stanton AV, Xu XY. Inter-individual variations in wall shear stress and mechanical stress distributions at the carotid artery bifurcation of healthy humans. *J Biomech.* 2002;35:1367-1377.

11. Krams R, Wentzel JJ, Oomen JA, Vinke R, Schuurbiers JC, de Feyter PJ, Serruys PW, Slager CJ. Evaluation of endothelial shear stress and 3D geometry as factors determining the development of atherosclerosis and remodeling in human coronary arteries *in vivo*. Combining 3D reconstruction from angiography and IVUS (ANGUS) with computational fluid dynamics. *Arterioscler Thromb Vasc Biol.* 1997;17:2061-2065.

12. Wentzel JJ, Whelan DM, van der Giessen WJ, van Beusekom HM, Andhyiswara I, Serruys PW, Slager CJ, Krams R. Coronary stent implantation changes 3-D vessel geometry and 3-D shear stress distribution. *J Biomech.* 2000;33:1287-1295.

13. Wentzel JJ, Krams R, Schuurbiers JC, Oomen JA, Kloet J, van Der Giessen WJ, Serruys PW, Slager CJ. Relationship between neointimal thickness and shear stress after Wallstent implantation in human coronary arteries. *Circulation.* 2001;103:1740-1745.

14. Wentzel JJ, Kloet J, Andhyiswara I, Oomen JA, Schuurbiers JC, de Smet BJ, Post MJ, de Kleijn D, Pasterkamp G, Borst C, Slager CJ, Krams R. Shear-stress and wall-stress regulation of vascular remodeling after balloon angioplasty: effect of matrix metalloproteinase inhibition. *Circulation.* 2001;104:91-96.

15. Krams R, Wentzel JJ, Cespedes I, Vinke R, Carlier S, van der Steen AF, Lancee CT, Slager CJ. Effect of catheter placement on 3-D velocity profiles in curved tubes resembling the human coronary system. *Ultrasound Med Biol.* 1999;25:803-810.

16. Krams R, Wentzel JJ, Oomen JA, Schuurbiers JC, Andhyiswara I, Kloet J, Post M, de Smet B, Borst C, Slager CJ, Serruys PW. Shear stress in atherosclerosis, and vascular remodelling *Semin Interv Cardiol*; 1998.

17. Bom N, de Korte CL, Wentzel JJ, Krams R, Carlier SG, van der Steen AW, Slager CJ, Roelandt JR. Quantification of plaque volume, shear stress on the endothelium, and mechanical properties of the arterial wall with intravascular ultrasound imaging. *Z Kardiol.* 2000;89:105-111.

18. Shah PK, Galis ZS. Matrix metalloproteinase hypothesis of plaque rupture: players keep piling up but questions remain. *Circulation.* 2001;104:1878-1880.

19. Galis ZS, Sukhova GK, Lark MW, Libby P. Increased expression of matrix metalloproteinases and matrix degrading activity in vulnerable regions of human atherosclerotic plaques. *J Clin Invest.* 1994;94:2493-2503.

20. Galis ZS, Johnson C, Godin D, Magid R, Shipley JM, Senior RM, Ivan E. Targeted disruption of the matrix metalloproteinase-9 gene impairs smooth muscle cell migration and geometrical arterial remodeling. *Circ Res.* 2002;91:852-859.

21. Lendon CL, Davies MJ, Born GV, Richardson PD. Atherosclerotic plaque caps are locally weakened when macrophages density is increased. *Atherosclerosis.* 1991;87:87-90.

22. Tronc F, Mallat Z, Lehoux S, Wassef M, Esposito B, Tedgui A. Role of matrix metalloproteinases in blood flow-induced arterial enlargement: interaction with NO. *Arterioscler Thromb Vasc Biol.* 2000;20:E120-126.

23. Palumbo R, Gaetano C, Melillo G, Toschi E, Remuzzi A, Capogrossi MC. Shear stress downregulation of platelet-derived growth factor receptor-beta and matrix metalloprotease-2 is associated with inhibition of smooth muscle cell invasion and migration. *Circulation.* 2000;102:225-230.

24. Pasterkamp G, Schoneveld AH, Hijnen DJ, de Kleijn DP, Teepen H, van der Wal AC, Borst C. Atherosclerotic arterial remodeling and the localization of macrophages and matrix metalloproteases 1, 2 and 9 in the human coronary artery. *Atherosclerosis.* 2000;150:245-253.

25. Shiomi M, Ito T, Hirouchi Y, Enomoto M. Fibromuscular cap composition is important for the stability of established atherosclerotic plaques in mature WHHL rabbits treated with statins. *Atherosclerosis.* 2001;157:75-84.

26. Korenaga R, Ando J, Kosaki K, Isshiki M, Takada Y, Kamiya A. Negative transcriptional regulation of the VCAM-1 gene by fluid shear stress in murine endothelial cells. *Am J Physiol.* 1997;273:C1506-1515.

27. Gonzales RS, Wick TM. Hemodynamic modulation of monocytic cell adherence to vascular endothelium. *Ann Biomed Eng.* 1996;24:382-393.

28. Truskey GA, Herrmann RA, Kait J, Barber KM. Focal increases in vascular cell adhesion molecule-1 and intimal macrophages at atherosclerosis-susceptible sites in the rabbit aorta after short-term cholesterol feeding. *Arterioscler Thromb Vasc Biol.* 1999;19:393-401.

29. Malinauskas RA, Sarraf P, Barber KM, Truskey GA. Association between secondary flow in models of the aorto-celiac junction and subendothelial macrophages in the normal rabbit. *Atherosclerosis.* 1998;140:121-134.

30. Buchanan JR, Jr., Kleinstreuer C, Truskey GA, Lei M. Relation between non-uniform hemodynamics and sites of altered permeability and lesion growth at the rabbit aorto-celiac junction. *Atherosclerosis.* 1999;143:27-40.

31. Long Q, Xu XY, Ramnarine KV, Hoskins P. Numerical investigation of physiologically realistic pulsatile flow through arterial stenosis. *J Biomech.* 2001;34:1229-1242.